Supporting Information

Cameron et al. 10.1073/pnas.1014743108

SI Methods

Contemporary Field Surveys of US Bumble Bees. During spring to fall seasons (April to October) of 2007–2009, we conducted intensive nationwide surveys of US bumble bee populations. In total, we sampled from 382 sites in 40 states (Fig. S1*A* and Table S1) and netted and identified a total of 9,006 bumble bees in the west and 7,832 in the east. Because it is difficult to predict areas that will have abundant bumble bees a priori, most survey sites were chosen opportunistically along roadsides by identifying areas with abundant floral resources, although site selection was also guided by historical specimen data and species distribution models (*SI Methods*, *Statistical Niche Models*). We divided the United States into western and eastern study regions, because the distribution of *Bombus* species is roughly split along the 104th western longitude, with the exception of certain nontarget species, such as *B. fervidus*, *B. griseocollis*, and *B. nevadensis*, that appear in both regions. All statistical analyses presented in this study were conducted separately for each region. After identifying a site and conducting a brief informal observation to confirm the presence of bumble bees, the site was typically surveyed for at least 0.5 person-h, with an average of ~1 ± 0.5 SD survey h per site. Surveys were conducted by walking back and forth through floral patches and collecting all observed bumble bees without consideration of species identity. Specimens were collected with aerial nets while in flight or while foraging at flowers; then, they were placed in vials and chilled on ice until the end of the collection period. Chilled specimens were identified to species using several identification tools, including color pattern guides, dichotomous keys (1–8), and other identification resources (http://www.life.illinois.edu/scameron/research/images/BumbleBeeFieldguide2010.pdf, http://beespotter.mste.uiuc.edu/topics/key/, http://www.nhm.ac.uk/research-curation/research/projects/bombus/_key_colour_world/Colour%20key%20to%20species%20for%20female%20bumblebees.html, and pinned reference collections). Unless identifications could not be determined in the field, specimens not belonging to the target species were generally released after identification to limit the impact of collecting on wild populations. In some cases, we collected additional specimens of abundant target species to increase sample sizes for genetic and pathogen analyses (*SI Methods*, *Pathogen Screening* and *SI Methods*, *Genetic Analysis*). Retained specimens from the eastern region were given unique identification codes and frozen in liquid nitrogen until returned to the University of Illinois, where they were maintained in liquid nitrogen or at −80 °C for genetic and pathogen screening. Western specimens were first killed in cyanide vials, dissected to remove gut tissue, and preserved dry until returned to the United States Department of Agriculture-Agricultural Research Service Pollinating Insect Research Unit in Logan, UT. Dissected gut tissue was frozen immediately in liquid nitrogen for pathogen analysis.

US Bumble Bee Natural History Collection Database. To understand the general patterns of historical relative abundance and distributions of the target species, we made use of the extensive natural history collections (NHC) of *Bombus* available at academic and government institutions throughout the United States. In some cases, records were obtained as electronic files directly from institutions, but most specimen data presented here are the result of our large-scale databasing effort between 2008 and 2010. Specimens were obtained through loans of all target species (including previously undetermined *Bombus*) from the institutions listed in Table S2. Species identity was confirmed with dichotomous keys (1–8) for all specimens by one of the authors or a trained technician. Collection-label data were entered into an electronic file. Specimens missing global positioning system (GPS) coordinate data were georeferenced using the digital tools Google Earth (http://earth.google.com/), TopoQuest (http://www.topoquest.com/), Earth Point (http://www.earthpoint.us), and Lat-Long.com (http://lat-long.com/). Locations of some reserves and parks were obtained from relevant government agency websites. Placement of coordinates for each specimen depended on the specificity of the collection-label data (e.g., county-level vs. populated place or other named geographic feature vs. distance and direction along a road from a populated place), and each record was given a qualitative accuracy score to aid in filtering for subsequent usage in distribution modeling. In total, we constructed a database of 77,991 *Bombus* specimens from 47 institutions, 73,759 of which were specimens of the eight target species. The specimens in this database represent much of the known continental US distributions of the target species as well as the temporal extent of each species' collection history (Fig. S1*B* and Table S2).

Statistical Niche Models. We predicted the potential ranges of the target species using the statistical niche modeling algorithm in the program MaxEnt v3.3 (9). MaxEnt uses presence-only locality data and random background points sampled from a study area to estimate the species distribution that is closest to uniform (subject to limited information on the true distribution and environmental conditions). Occurrence data were obtained from the US bumble bee database described above. We examined and filtered records, using only specimens identified by ourselves or a trusted expert and for which we could confidently specify geographical coordinates. This resulted in 2,063 locality records for *B. affinis*, 2,546 for *B. bimaculatus*, 6,822 for *B. impatiens*, 5,903 for *B. pensylvanicus*, 3,667 for *B. terricola*, 4,262 for *B. bifarius*, 3,302 for *B. occidentalis*, and 1,960 for *B. vosnesenskii*, which covered most of the known US range of each species. If multiple records occurred within the same environmental grid cell (5-min resolution) or fell outside of the geographic extent considered for this study, they were excluded during analysis. Environmental data were obtained from a set of 19 bioclimatic variables in the WorldClim 1.3 dataset (10). These variables summarize annual averages, seasonality, and extremes of temperature and precipitation that have been interpolated from global weather stations and are averaged over a period ranging from ~1950 to 2000. To limit the number of variables used for modeling, we calculated Pearson's correlation coefficient (r) between each pair of the 19 WorldClim variables for 1,000 randomly selected points from the geographic extent used for modeling. Correlations were assessed separately for the east and west. For each comparison with $|r| \geq 0.90$, we selected one variable for modeling. For the eastern species, selected variables were annual mean temperature, mean diurnal range, isothermality, maximum temperature of the warmest month, temperature annual range, mean temperature of the wettest quarter, mean temperature of the driest quarter, annual precipitation, precipitation of the wettest month, precipitation seasonality, and precipitation of the warmest quarter. For the western species, variables were annual mean temperature, mean diurnal range, isothermality, temperature seasonality, maximum temperature of the warmest month, minimum temperature of the coldest month, mean temperature of the wettest quarter, mean temperature of the driest quarter, annual precipitation, precipitation of the driest month, precipitation seasonality, and precipitation of the warmest quarter. However, it should be noted that the variables selected made little difference in the resulting maps. MaxEnt

models were trained separately for the eastern and western regions. We averaged models over 50 replicates using a random 80% subset of localities to train the model and 20% reserved for testing using the area under the receiver operating curve (AUC) statistic.

Overall, the niche models (Fig. 1) produced by MaxEnt generally reflect what is known of the historical range of these species (4, 8, 11, 12). AUC values generally indicated good model performance (all test AUC values > 0.80 averaged over 50 subsampled MaxEnt runs) except for *B. pensylvanicus* (AUC = 0.731 ± 0.015 SD) (Table S3). However, the distribution of *B. pensylvanicus* covers the vast majority of the geographic extent used for modeling. Because MaxEnt is a presence-only modeling method, true absences are not used to estimate commission errors when plotting the receiver operating characteristic curve, but rather, pseudoabsence points are randomly sampled from the predicted distribution (9). When a species has a large area of occurrence, the maximum achievable AUC will be well below unity (in the case of *B. pensylvanicus*, this expected maximum value is 0.699 ± 0.003 SD, although this can be exceeded in practice). Thus, the observed AUC for *B. pensylvanicus* likely reflects the very large area of occurrence for this bumble bee, as observed in the NHC data (Fig. S1*B*), rather than poor model performance. Our models should, therefore, represent good approximations for areas where we would expect the target species to occur given historical information about their occurrences.

Comparisons of Historical and Contemporary Collections. When inferring temporal changes in abundance and distribution of most organisms, biases exist in the collection records. Nonetheless, we wanted to compare the relative abundance of the eight target species in our standardized surveys (2007–2009) to their historical relative abundances in the NHC database. To minimize bias, we analyzed the data at broad geographic and temporal scales. Only target species were used in the relative abundance estimates (i.e., nontarget species identified from surveys and NHC were not included in the total species counts).

We pooled specimen data from 1900 to 1999 from the US bumble bee NHC database to represent historical abundances for the six target species. We excluded data from 2000 to 2006 because of generally low collection efforts documented in NHC (Table S2) during this time frame. It should also be noted that, between 2000 and 2006, declines of some western bumble bees were being documented in North America (13), and therefore, including data from this period could confound our calculations of historical abundances. We excluded specimen data before the 1900s because of spotty collection histories and overly generalized locality information (e.g., Utah and Northwest Territory). Considering the temporal depth (100 y) (Table S2) and geographic breadth (~10,000 historic collection locations) (Fig. S1*B* and Table S2) representing the abundance of each target species, we make the assumption that the collection history of each NHC is not strongly biased to any one species. In our analysis, we excluded historical records from states in which we did not conduct standardized surveys (Delaware, Florida, Maryland, Michigan, New Hampshire, New Jersey, Rhode Island, and West Virginia).

We partitioned the relative abundance analysis into four regional categories, because three of eight target bumble bee species have restricted geographic distributions: global west, *B. bifarius* and *B. occidentalis*; Pacific west, *B. bifarius*, *B. occidentalis*, and *B. vosnesenskii*; global east, *B. bimaculatus*, *B. impatiens*, and *B. pensylvanicus*; northern/coastal east, *B. affinis*, *B. bimaculatus*, *B. impatiens*, *B. pensylvanicus*, and *B. terricola* (Fig. 2 lists all states included). We calculated relative abundance for each regional category as the number of individuals collected for each target species divided by the total number of respective targets collected in a given region. We used *z* tests of equal proportions (*Methods*) to compare relative abundances.

We also used predictions from our MaxEnt models (Fig. 1) in an additional assessment of decline. We set a relatively strict logistic probability presence threshold of 0.20 to create binary presence–absence raster layers, which produced conservative (i.e., omitted a number of actual survey observations for each species) but reasonably realistic distribution maps for the eight target species. For each species, if a current survey site fell within the threshold distribution, we specified that locality as an expected presence (any actual occurrences omitted because of the conservative threshold were added to this presence class) and calculated the fraction of those sites where we actually observed the species (Table S4).

Finally, to obtain estimates of range losses for declining species within our surveyed study areas, we used MaxEnt niche models together with minimum convex polygons (MCPs) constructed for species occurrences in historical records and contemporary surveys. First, to approximate our areas of study for both east and west regions, we used the ArcView 9.2 (ESRI) extension Hawth's Tools (14) to calculate MCPs around all 2007–2009 survey sites. For each target species, we then extracted all historical records from the NHC database that fell within the boundaries of these polygons and constructed MCPs for these historical localities as well as for occurrences within our contemporary surveys. Although it would be possible to analyze these MCPs alone to determine percent range loss observed for our surveys, in most cases, their boundaries covered geographic regions unlikely to be inhabited by a given species. To improve our estimates, we, thus, excluded regions with low probability of species occurrence by overlaying the historical and contemporary MCPs with the binary presence–absence MaxEnt maps (see above). This niche model-based constraint improved overestimates of range loss compared with the use of uncorrected MCPs (see below) (Table S5). The percent range remaining for each species was estimated by dividing the areas (total number of 5-min resolution pixels) of the niche model-constrained contemporary and historical MCPs. We observed some degree of range loss for all species (Table S5), not only for the hypothesized declining species (loss ranging from 34% to 98%) but also for those that our surveys indicate are abundant and widespread (loss of 5–11%). We expect that this result reflects both the sparser survey densities at the edges of our study areas and the much more numerous historical localities available for each species. We, thus, used the most severe range loss (11%) observed for a stable species (*B. bifarius*) to approximate the degree to which range loss is overestimated in our analysis because of sampling effects (Table S5).

Pathogen Screening. We examined dissected midgut tissues of target *Bombus* species to determine the presence of infection by *Nosema bombi*. Infections were recognized by presence of mature infective spores that develop in the cytoplasm of cells in the tissues. The spores are oval, ~2 × 4 μm in size, and brightly refractive under phase-contrast microscopy. We dissected western *Bombus* specimens in the field or in the laboratory in Logan, UT, and shipped the digestive tracts on dry ice to the insect pathogen laboratory at the Illinois Natural History Survey. We placed the collected eastern *Bombus* specimens on ice or directly into liquid nitrogen shipping tanks and stored the samples in the laboratory at −80 °C. Specimens were thawed and dissected immediately before screening for *N. bombi*.

Microscopic examination of pathogen prevalence. We removed midgut tissues from the abdomens of collected bees, smeared fresh tissue samples on glass microscope slides, and screened for pathogens using phase-contrast microscopy at 400× magnification. Dissection tools were sterilized between samples. We determined presence/absence of *N. bombi* spores by inspecting an area of 4 × 5 visual fields (20 visual fields per tissue smear) on a slide. For light infections or smears that were difficult to evaluate, additional tissue was prepared for repeated screenings. We determined prevalence of infection for each host population (individual hosts infected per

Bombus species per site). To assess significant among-species differences in the proportion of infected individuals per collection site, we used generalized linear models for weighted binomial proportion data (Table S6) implemented in R v2.10.1 (15).

Pathogen infection intensity. To determine total production of mature *N. bombi* spores in the midgut of a host, we homogenized the tissues in a tissue grinder with 100 μL water and determined the spore count per microliter suspension using a Petroff-Hauser hemocytometer. High-intensity infections were visible under the microscope as very dense layers of spores, whereas light infections often were detected at less than 20 spores per slide. We recorded the average number of spores per visual field to represent infection intensity in the entire gut of each individual. Based on repeated spore counts of low-, medium-, and heavy-infected gut tissues determined by visual inspection, we defined the levels of infection intensity as follows: low infection, an average of <2 spores per visual field = 1–1,000 spores/μL; moderate infection, 2–20 spores/visual field = 1,000–100,000 spores/μL; high infection, >20 spores/visual field ≥ 100,000 spores/μL. We did not perform statistical analysis of infection intensity because of the small number of infections outside of *B. pensylvanicus* and *B. occidentalis*, and high-intensity infections were much more common in these two species: spore counts for 38.6% and 64% of all infections, respectively, were higher than 100,000 spores/μL. With the exception of *B. vosnesenskii*, in which 33.3% of infections (although in only 4 out of 12) were heavy, all other species had less than 20% heavy infections, and there were no high-level infections in *B. bimaculatus*.

Genetic assessment. We determined the species identity of observed microsporidian infections using DNA sequencing. To extract DNA from infected midgut tissues of a set of representative *Bombus* individuals, we added tissue samples to 150 μL 5% Chelex 100 resin (Bio-Rad) and 5 μL *proteinase K* (20 mg/mL). The sample was incubated at 55 °C for 1 h followed by 95 °C for 15 min to denature the enzyme. DNA was available in the supernatant after a short centrifugation. Samples were stored at −20 °C until needed. PCR was carried out using the oligonucleotide primers 1061f (16), 228r, 530f, r (17), SSUres-f1/r1 (18), 18f, 1492r, and 1047r (19) to amplify portions of the small subunit, large subunit, or internal transcribed spacer regions of the ribosomal RNA. Reactions were generally performed with 25-μL samples containing 4 μL DNA, 5 μL 5× Promega GoTaq flexi buffer, 2 μL 25 mM $MgCl_2$, 0.5 μL dNTPs (10 mM each), 0.125 μL 5 U GoTaq polymerase (Promega), and 2.5 μL of each forward and reverse primer (2.5 μM). The PCR parameters were initial DNA template denaturing at 95 °C for 3 min and 35 cycles of denaturation at 95 °C for 45 s; primer annealing temperature ranged from 48 °C to 56 °C for 30 s, and primer extension was at 72 °C for 90 s followed by a final extension at 72 °C for 5 min. To determine the microsporidian species in the gut, the PCR product was purified using ExoSAP-IT (Affymetrix) and sequenced on an ABI 3730xl capillary sequencer (Applied Biosystems) at the University of Illinois Core Facility sequencing center. Resulting sequences were identical to European strains of *N. bombi* and are available in GenBank as accession nos. HM142724–HM142729 and HM173334–HM173341 (Table S7).

Genetic Analysis. ***DNA extraction.*** Specimens for genetic analysis were collected from April to October of 2007–2009 throughout the United States (see above). We extracted DNA from 664 *B. impatiens* worker specimens from 38 sample sites, 534 *B. bimaculatus* from 43 sites, 455 *B. pensylvanicus* from 52 sites, 479 *B. vosnesenskii* from 19 sites, 630 *B. bifarius* from 38 sites, and 115 *B. occidentalis* from 31 sites (Table S8). For final analyses, sample sites were pooled into regional subpopulations where limited specimens were available (Table S8). This did not seem to impact results, especially considering the low levels of genetic differentiation observed for most species and the minimal deviations from Hardy–Weinberg and linkage equilibria, even in pooled subpopulations (see below). DNA was extracted from frozen or pinned specimens using a modified Chelex protocol (20, 21). Extractions were preserved at −20 °C.

Microsatellite genotyping. The three eastern target species (*B. impatiens*, *B. bimaculatus*, and *B. pensylvanicus*) were genotyped at 11 microsatellite loci (B10, B96, B121, B126, B124, BL13, BL15, BT10, BT28, BT30, and BTERN01), and western target species (*B. vosnesenskii*, *B. bifarius*, and *B. occidentalis*) were genotyped at 10 loci (B10, B96, B116, B119, B124, BL11, BL13, BT10, BT28, and BTERN01); all loci were identified from the literature (22–24). The B121 locus amplified weakly and unreliably in *B. impatiens*, as did B10 and B119 in *B. vosnesenskii*, B10 in *B. bifarius*, and B116 in *B. occidentalis*; these loci were excluded from analysis for these species. PCR amplifications were conducted in 10-μL volumes with 2 μL 5× GoTaq flexi buffer, 1.875 mM $MgCl_2$, 0.2 mM each dNTP, 0.08–0.5 μM each primer (forward labeled with VIC, NED, 6-FAM, or PET dyes, reverse unlabeled; Applied Biosystems), and 0.4 units GoTaq polymerase with 0.5–2 μL genomic DNA. Typical thermal cycling conditions were 94 °C for 2 min and 30 cycles of 94 °C for 30 s, 48–52 °C for 30 s, and 72 °C for 30 s followed by an extension cycle of 72 °C for 45 min, with adjustments made depending on the quality of initial amplification results. Electrophoresis for eastern species was performed on ABI 3730xl capillary DNA sequencers (Applied Biosystems) at the high-throughput DNA facility at the University of Illinois W. M. Keck Center for Comparative and Functional Genomics, and electrophoresis for western species was performed on ABI 3730xl capillary DNA sequencers at the Utah State University Center for Integrated BioSystems core facility. Alleles were scored manually using GENEMAPPER 4.3 (Applied Biosystems) with separate bin sets for each species. There was no evidence of amplification or scoring error based on repeat genotyping of subsets of individuals for each species.

Genetic data analysis. Bumble bees live socially in colonies, and when collecting workers at a given site, it is possible to sample multiple sisters from the same colony (full sibs), potentially affecting estimates of population genetic parameters (25). For each species, we identified sisters using a full-maximum likelihood approach for monogamous haplodiploids implemented in COLONY 2.0 (26). Population allele frequencies for each species were estimated from the complete dataset, and only workers from the same sample sites were considered as potential sibs. Because no evidence of error was detected from replicate genotyping of individuals and we excluded all problematic markers (see below), we specified a relatively low probability of null alleles and other errors (0.5% per locus). In practice, the precise value of these probabilities did not alter results in preliminary assessments. For each full-sib group, one individual was randomly chosen to represent the colony in subsequent genetic analyses.

The final datasets were tested for deviations from Hardy–Weinberg and linkage equilibria using GENEPOP v4.0 (27). Deviations from Hardy–Weinberg equilibrium (HWE) were tested with a Markov chain approximation to an exact (significance) test, whereas significant linkage disequilibrium (LD) was assessed with likelihood ratio tests; in both cases, Bonferroni corrections were applied. Only two locus by subpopulation comparisons were significant for deviations from HWE for the eastern *Bombus* species: locus BL15 in impNCb (Mt. Mitchell, NC) in *B. impatiens* and B121 in penMOKS (a pool of three sites in southwest Missouri and southeast Kansas) in *B. pensylvanicus*. *B. bimaculatus* exhibited significant LD for BL13 + BT10 in bimSD and for B121 + BT10 and BL15 + BT10 in bimWIc. For *B. impatiens*, LD was significant for BL15 + BT10 in impALa, B10 + BL15 in impOH, and B10 + BL15 in impWIa. There was no LD detected for *B. pensylvanicus*. In the west, *B. bifarius* showed highly significant deviations from HWE at B119 in all subpopulations, and therefore, this locus was excluded from further analysis. There were no

HWE deviations in *B. vosnesenskii* or *B. occidentalis* and no significant LD in any western species. Overall, the low number of significant values across all species suggests that HWE deviations and LD are not a major problem for this dataset.

We used FSTAT v2.9.3.2 (28) to estimate global genetic structure among populations using F_{ST} (29), with 95% confidence intervals estimated by bootstrapping loci and significance of genotypic differentiation among populations estimated using 1,000 permutations of genotypes among populations. We also estimated Jost's D (30), a statistic that provides a true measure of differentiation for highly variable markers, such as microsatellites, using the software SMOGD v2.6 (31). Finally, in an attempt to identify well-defined genetic groups that might be useful for diagnosing evolutionarily significant management units (32), we examined population structure with the Bayesian clustering algorithm implemented in STRUCTURE v2.3.3 (33). The STRUCTURE model assumes that a sample of individuals comprises K potential populations, to which individual genotypes (or fractional genotypes) can be assigned. We used default parameter settings to assign individuals to populations (allowing for correlated allele frequencies and admixture), with 20,000 burn-in steps followed by 50,000 samples, and evaluated results over a range of K values. For the purposes of this study, we limit results to $K = 3$ to illustrate an overall presence or lack of genetic structure; detailed results will be presented in a companion paper. All results were stable across multiple runs.

For each species, we estimated average expected genetic variation and interlocus SE per subpopulation and in total (i.e., all individuals pooled) using Nei's measure of gene diversity (H_E) (34). Significance levels of pair-wise differences in H_E among species were estimated using 1,000 subpopulation-level randomizations in FSTAT v2.9.3.2 (only loci shared by all species within each region were included in the test). We also tested for differences in the proportion of unique colonies to total specimens collected per site (as identified by COLONY; excluding sites with only one individual of a given species) among species in each region using generalized linear models with quasibinomial errors and a logit link function in R v2.10.1 (Table S9).

1. Williams PH, Cameron SA, Hines HM, Cederberg B, Rasmont P (2008) A simplified subgeneric classification of the bumblebees (genus *Bombus*). *Apidologie (Celle)* 39: 46–74.
2. Stephen WP (1957) *Bumble Bees of Western America* (Oregon State College, Agricultural Experiment Station, Corvalis, OR), Technical Bulletin.
3. LaBerge WE, Webb MC (1962) *The Bumblebees of Nebraska* (University of Nebraska College of Agriculture, Agricultural Experiment Station, Lincoln, NE), Research Bulletin.
4. Mitchell TB (1962) *Bees of the Eastern United States II (Megachilidae, Anthophoridae, Apidae ss)* (North Carolina Agricultural Experiment Station, Raleigh, NC), Technical Bulletin.
5. Medler JT, Carney DW (1963) *Bumblebees of Wisconsin (Hymenoptera: Apidae)* (University of Wisconsin, Madison, WI), Research Bulletin.
6. Chandler L, McCoy CE, Jr. (1965) The bumble bees of Arkansas (Hymenoptera, Apidae, Bombinae). *Proc Arkansas Acad Sci* 19:46–53.
7. Husband RW, Fischer RL, Porter TW (1980) Description and biology of bumblebees (Hymenoptera: Apidae) in Michigan. *Great Lakes Entomol* 13:225–239.
8. Thorp RW, Horning DS, Dunning LL (1983) *Bumble Bees and Cuckoo Bumble Bees of California (Hymenoptera: Apidae),* Bulletin of the California Insect Survey (University of California Press, Berkeley and Los Angeles, CA).
9. Phillips SJ, Anderson RP, Schapire RE (2006) Maximum entropy modeling of species geographic distributions. *Ecol Model* 190:231–259.
10. Hijmans RJ, Cameron SE, Parra JL, Jones PG, Jarvis A (2005) Very high resolution interpolated climate surfaces for global land areas. *Int J Climatol* 25:1965–1978.
11. Milliron HE (1971) A monograph of the western hemisphere bumblebees (Hymenoptera: Apidae; Bombinae). I. The genera *Bombus* and *Megabombus* subgenus *Bombias*. *Mem Entomol Soc Can* 82:1–80.
12. Milliron HE (1973) A monograph of the western hemisphere bumblebees (Hymenoptera: Apidae; Bombinae). II. The genus *Megabombus* subgenus *Megabombus*. *Mem Entomol Soc Can* 89:81–237.
13. Thorp RW, Shepherd MD (2005) *Subgenus Bombus. Latreille, 1802 (Apidae: Apinae: Bombini).* Available at www.xerces.org/Pollinator_Red_List/Bees/Bombus_Bombus.pdf. Accessed December 14, 2010.
14. Beyer HL (2004) *Hawth's Analysis Tools for ArcGIS.* Available at http://www.spatialecology.com/htools. Accessed December 14, 2010.
15. R Development Core Team (2009) *R: A Language and Environment for Statistical Computing* (R Foundation for Statistical Computing, Vienna).
16. Weiss LM, Vossbrinck CR (1998) Microsporidiosis: Molecular and diagnostic aspects. *Adv Parasitol* 40:351–395.
17. Vossbrinck CR, Baker MD, Didier ES, Debrunner-Vossbrinck BA, Shadduck JA (1993) Ribosomal DNA sequences of *Encephalitozoon hellem* and *Encephalitozoon cuniculi*: Species identification and phylogenetic construction. *J Eukaryot Microbiol* 40:354–362.
18. Klee J, et al. (2007) Widespread dispersal of the microsporidian *Nosema ceranae*, an emergent pathogen of the western honey bee, *Apis mellifera*. *J Invertebr Pathol* 96:1–10.
19. Vavra J, et al. (2006) *Vairimorpha disparis* n. comb. (Microsporidia: Burenellidae): A redescription and taxonomic revision of *Thelohania disparis* Timofejeva 1956, a microsporidian parasite of the gypsy moth *Lymantria dispar* (L.) (Lepidoptera: Lymantriidae). *J Eukaryot Microbiol* 53:292–304.
20. Lozier JD, Cameron SA (2009) Comparative genetic analyses of historical and contemporary collections highlight contrasting demographic histories for the bumble bees *Bombus pensylvanicus* and *B. impatiens* in Illinois. *Mol Ecol* 18:1875–1886.
21. Strange JP, Knoblett J, Griswold T (2009) DNA amplification from pin-mounted bumble bees (*Bombus*) in a museum collection: Effects of fragment size and specimen age on successful PCR. *Apidologie (Celle)* 40:134–139.
22. Estoup A, Scholl A, Pouvreau A, Solignac M (1995) Monoandry and polyandry in bumble bees (Hymenoptera; Bombinae) as evidenced by highly variable microsatellites. *Mol Ecol* 4: 89–93.
23. Estoup A, Solignac M, Cornuet J-M, Goudet J, Scholl A (1996) Genetic differentiation of continental and island populations of *Bombus terrestris* (Hymenoptera: Apidae) in Europe. *Mol Ecol* 5:19–31.
24. Reber Funk C, Schmid-Hempel R, Schmid-Hempel P (2006) Microsatellite loci for *Bombus* spp. *Mol Ecol Notes* 6:83–86.
25. Anderson EC, Dunham KK (2008) The influence of family groups on inferences made with the program Structure. *Mol Ecol Res* 8:1219–1229.
26. Jones O, Wang J (2009) COLONY: A program for parentage and sibship inference from multilocus genotype data. *Mol Ecol Res* 10:551–555.
27. Rousset F (2008) Genepop'007: A complete reimplementation of the Genepop software for Windows and Linux. *Mol Ecol Res* 8:103–106.
28. Goudet J (2001) *fstat, a Program to Estimate and Test Gene Diversities and Fixation Indices, version 2.9.3.* Available at http://www.unil.ch/popgen/softwares/fstat.htm. Accessed December 14, 2010.
29. Weir BS, Cockerham CC (1984) Estimating *F*-statistics for the analysis of population structure. *Evolution* 38:1358–1370.
30. Jost L (2008) G_{ST} and its relatives do not measure differentiation. *Mol Ecol* 17: 4015–4026.
31. Crawford NG (2010) SMOGD: Software for the measurement of genetic diversity. *Mol Ecol Res* 10:556–557.
32. Palsbøll PJ, Bérubé M, Allendorf FW (2007) Identification of management units using population genetic data. *Trends Ecol Evol* 22:11–16.
33. Pritchard JK, Stephens M, Donnelly P (2000) Inference of population structure using multilocus genotype data. *Genetics* 155:945–959.
34. Nei M, Kumar S (2000) *Molecular Evolution and Phylogenetics* (Oxford University Press, New York).

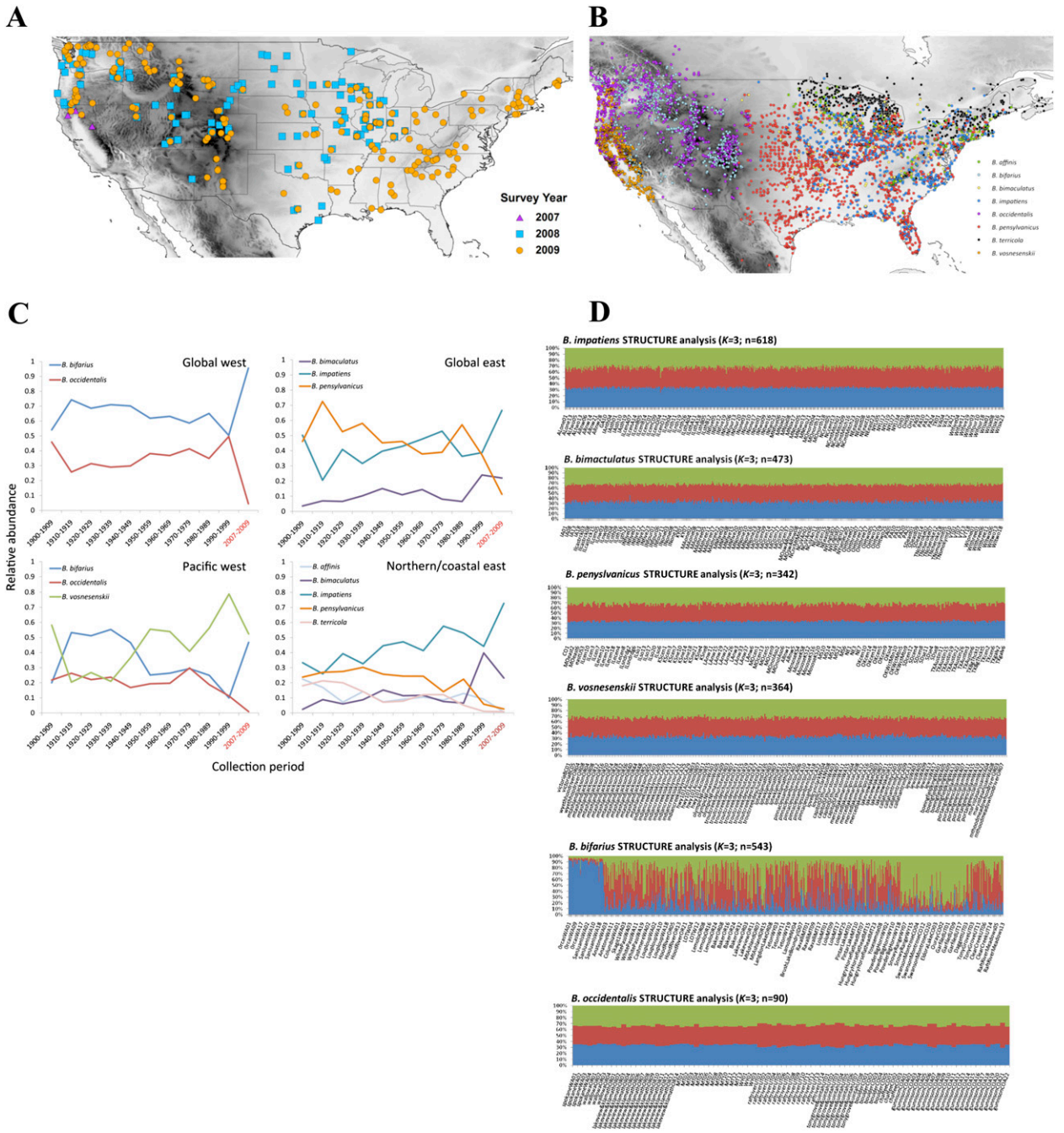

Fig. S1. (*A*) Map of the 382 sites surveyed for *Bombus* from 2007 to 2009 (see Table S1 for details). (*B*) Digitized natural history collection records for the eight target *Bombus* species (see Table S2 for a detailed summary). (*C*) Temporal trends in relative abundance for each target *Bombus* species in four regional comparisons (Fig. 2). Data for 1900–1999 (black axis labels; specimens pooled by decade) were taken from the *Bombus* natural history collections database (*B* and Table S2) and for 2007–2009 (red axis labels), from field surveys (*A*) (Table S1). Plots of historical and contemporary relative abundances are consistent with recent declines for the less abundant bumble bee species over the last 20–30 y, with our 2007–2009 surveys recovering proportionally fewer specimens of *B. affinis*, *B. occidentalis*, *B. pensylvanicus*, and *B. terricola* than in any decade of the 20th century. (*D*) Selected results from STRUCTURE analyses of six genotyped *Bombus* species. Each vertical bar represents a single sample taken from throughout the range of each species (*x* axis) (Table S8). The *y* axis indicates the proportion of an individual's genotype assigned to a particular genetic cluster (each cluster shown as a unique color). Only *B. bifarius* shows any evidence of genetic structure. All individuals in each of the other species are assigned equally to the three clusters, indicating a lack of subspecies or other major genetic subdivisions. For simplicity, only $K = 3$ is shown; the same results seem to hold for any specified K. Detailed results will be the subject of a companion paper.

Other Supporting Information Files

Table S1 (DOC)
Table S2 (DOC)
Table S3 (DOC)
Table S4 (DOC)
Table S5 (DOCX)
Table S6 (DOC)
Table S7 (DOC)
Table S8 (DOCX)
Table S9 (DOC)